PROCEEDINGS OF SCIENCE

Gamma-gamma absorption in γ-ray binary systems

DC du Plooy* **and B van Soelen**
Department of Physics, University of the Free State, PO Box 339, Bloemfontein 9300, South Africa
E-mail: duplooydc@ufs.ac.za

Gamma-ray binaries are a subclass of high-mass binary systems and are generally distinguished by their spectral energy distributions peaking above 1 MeV. Gamma-ray binaries consist of an O or B type star and an orbiting compact object which is either a neutron star or a black hole. The nature of the compact object in γ-ray binaries remains unknown except for two systems, namely PSR B1259-63 and PSR J2032+4127, where the compact objects have been identified as pulsars. In the case of a neutron star compact object, the very high energy (VHE) emission mechanism is believed to originate from the interaction between the stellar and pulsar winds. Generally, γ-ray binary light-curves show that the maximum in the GeV and TeV emission occurs at different orbital phases, with the maximum GeV emission occurring at superior conjunction and the maximum TeV emission occurring at inferior conjunction. Therefore, $\gamma\gamma$ absorption might prove useful in constraining the TeV emission region by studying how it affects the observed spectrum. We have calculated the $\gamma\gamma$ absorption in six of the seven known γ-ray binaries and the results are presented in this paper.

7th Annual Conference on High Energy Astrophysics in Southern Africa - HEASA2019
28 - 30 August 2019
Swakopmund, Namibia

*Speaker.

PoS(HEASA2019)054

1. Introduction

Gamma-ray binaries are a subclass of high-mass binary systems and consist of a compact object, either a neutron star or a black hole, in orbit around an O or B type star. Gamma-ray binaries show emission up to TeV energies, produced by the inverse Compton scattering of electrons off stellar photons. Generally in these systems the nature of the compact object remains unknown, except for two sources, namely PSR B1259-63 and PSR J2032+4127, where the compact objects have been identified as pulsars [1, 2, 3]. In the case of a neutron star compact object, the neutron star is most likely a young pulsar which is spinning too rapidly for accretion to occur. Accretion of material onto the poles of a neutron star would short out the electric field responsible for pulsed radio emission, which contradicts the detections made in the two aforementioned γ-ray binary systems. However, the possibility of a microquasar scenario is still open to debate for the other systems, in which case the γ-rays would be produced via Compton scattering close to the base of the relativistic jet [4, 5]. In the case of a pulsar compact object, the winds originating from the pulsar and companion star produce a shock situated between the two orbiting bodies and due to the stellar wind domination over the pulsar wind, the shock structure takes the shape of a cometary tail flowing over the pulsar. At the apex of the shock high energy particles are accelerated to VHE similarly to pulsar wind nebulae as described by e.g. Gaensler & Slane [6]. However, due to the dense photon field the resulting $\gamma\gamma$ absorption will also be high [7]. A second possible location for the emission has been discussed, situated further along the cometary tail, at the Coriolis turnover [8, 9, 10]. In this paper we include results on measuring the level of $\gamma\gamma$ absorption in γ-ray binaries by constructing absorption maps. These absorption maps provide valuable insight that will be used to place constraints on where the observed VHE emission can originate from.

2. Theory

Gamma-ray photons will undergo $\gamma\gamma$ absorption in the photon field of the star when

$$E_\gamma \epsilon \geq \frac{2m_e^2 c^4}{(1-\vec{e_\gamma}\cdot\vec{e_\star})} \tag{2.1}$$

where E_γ is the energy of the γ-ray, ϵ is the energy of the optical target photon, m_e is the electron mass, c is the speed of light, and $\vec{e_\gamma}$ and $\vec{e_\star}$ are the direction of motion of the γ-ray and optical photon respectively. Following the description in Dubus [7], the opacity of a γ-ray photon produced with energy in the binary system, travelling in a direction $\vec{e_\gamma}$, can be described by a quadruple integral which is dependent on the path length ℓ, the solid angle over the star $d\Omega = d\mu d\phi$ (where $\mu = \cos\theta$; refer to Fig. 1) , and the energy of the target photon, ϵ, and can be written as

$$\tau_{\gamma\gamma} = \int_0^\infty \int_{\mu_{\min}}^1 \int_0^{2\pi} \int_{\epsilon_{\min}}^{\epsilon_{\max}} n_\epsilon \sigma_{\gamma\gamma}(1-\vec{e_\gamma}\cdot\vec{e_\star})\, d\epsilon d\phi d\mu d\ell \tag{2.2}$$

where n_ϵ is the stellar photon number density, $\sigma_{\gamma\gamma}$ is the interaction cross-section, $\mu_{\min} = \sqrt{(1-(R_\star/d)^2)}$, d is the distance to the centre of the star. The $\gamma\gamma$ cross-section is given

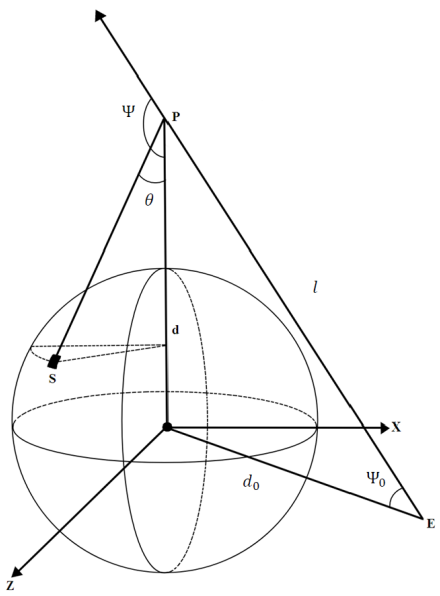

Figure 1: The geometry of the γ-ray and stellar photon interaction where the sphere represents the optical companion. The emission region of the γ-ray photon is given by E, a distance d_0 from the centre of the star. The γ-ray photon travels a distance ℓ before it interacts with the stellar photon, which is produced at S. The angles Ψ_0, Ψ and θ represent the γ-ray emission angle, the interaction angle, and the co-latitude respectively.

by [11]

$$\sigma_{\gamma\gamma} = \frac{3}{16}\sigma_{\mathrm{T}}(1-\beta^2)\left[(3-\beta^4)\ln\left(\frac{1+\beta}{1-\beta}\right) - 2\beta(2-\beta^2)\right], \tag{2.3}$$

where σ_{T} is the Thomson cross-section and β is a unit-less parameter given by

$$\beta = \sqrt{1 - \frac{2m_e^2c^4}{\epsilon E_\gamma(1-\vec{e_\gamma}\cdot\vec{e_\star})}}. \tag{2.4}$$

3. Results

Maps of the level of $\gamma\gamma$ absorption for $E_\gamma = 1$ TeV are shown in Fig. 2 with the observer positioned at the bottom of the figure. The colour gradient shows the level of absorption. These maps were constructed by determining the absorption, using equation 2.2, and constrained to within a multiplication of five times the original orbit size. The binary parameters are listed in Table 1.

4. Discussion & Conclusions

Generally, because of the high angular dependence of inverse Compton scattering what is expected is that the maximum GeV and TeV emission occurs near or at superior

Table 1: Binary parameters used in the model. The parameters are described as follows; $P_{\rm orb}$ is the orbital period, e is the eccentricity, ω is the argument of periastron, i is the orbital inclination, $T_\star$ is the effective stellar surface temperature, $R_\star$ is the stellar radius, $M_\star$ is the companion stellar mass, and $M_{\rm compact}$ is the compact object mass. Where values are constrained by observations the error is also reported in brackets.

	LS 5039 $^{\bowtie}$	**PSR B1259-63** †	**LS I 61° 303** *	**1 FGL J1018.6-5856** *	**HESS J0632+057** ‡	**LMC P3** $^{\diamond}$
$P_{\rm orb}$ (days)	3.90603(8)	1236.724526(6)	26.496(3)	16.544(8)	315(5)	10.301(2)
e	0.24(8)	0.86987970(6)	0.54(3)	0.31	0.83(8)	0.40(7)
ω (°)	212(5)	138.665013(11)	41(6)	89(30)	129(17)	11(12)
i (°)	64	$153.3^{+3.2}_{-3.0}$	60	64	80	50
$T_\star$ (K)	39000	33500	22500	38900	30000	40000
$R_\star$ ($R_\odot$)	9.3	9.2	10	10.1	8	15
$M_\star$ ($M_\odot$)	23	29.8	12	31	16	42
$M_{\rm compact}$ ($M_\odot$)	1.4	1.4	1.4	1.4	1.4	1.4

$\bowtie$ [12, 13, 14]; † [15, 16, 17]; $\star$ [13, 18]; $*$ [19, 20, 21]; ‡ [22, 23, 24]; $\diamond$ [25, 26, 27]

conjunction. However, if the VHE photons exceed the energy threshold for $\gamma\gamma$ absorption this will affect the observed TeV spectrum. As can be seen in figure 1, the majority of the $\gamma\gamma$ absorption occurs directly behind the companion star, relative to an observer positioned below the figure. This would result in the γ-ray photons travelling towards the observer to encounter a much denser photon field. Therefore because of the higher amount of $\gamma\gamma$ absorption of TeV photons at superior conjunction, what is observed is that the maximum GeV emission occurs at superior conjunction while the maximum TeV emission occurs at inferior conjunction. This can explain the difference between the GeV and TeV light-curves, in systems like LS 5039 and LMC P3 [7, 28, 27]. Other than the high angular dependency, $\gamma\gamma$ absorption is also highly dependent on the binary separation. By comparing LS 5039 and HESS J0632+057 one can see that for closely separated binary systems, a significant degree of absorption still occurs at or near inferior conjunction. In γ-ray binaries, $\gamma\gamma$ absorption will result in a decrease in the observed flux and will harden the TeV spectrum because the absorption will be highest in the around at few 100s of GeV energies. The $\gamma\gamma$ calculations discussed here will be used to predict how the flux and the photon index will change during the orbit for emission originating at different distances along the bow shock. The main objective of this study is to produce predictions that can constrain the possible locations of the TeV emission and which can be tested with the upcoming Cherenkov Telescope Array.

Acknowledgments

The numerical calculations were performed using the University of the Free State High Performance Computing Unit.

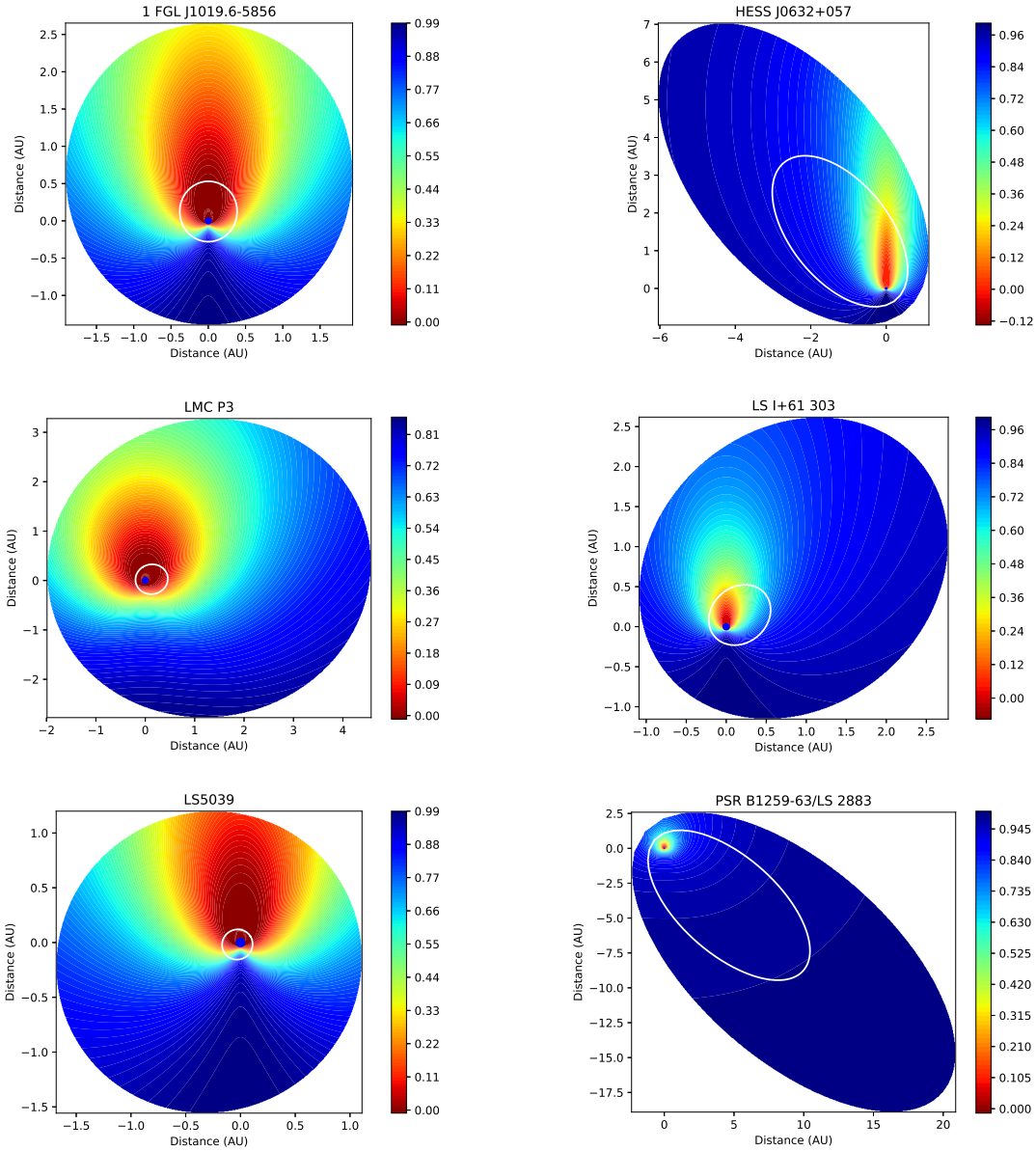

Figure 2: The absorption maps around the γ-ray binaries for a 1 TeV γ-ray photon for an observer positioned at the bottom of the page. The orbit of the compact object is given by a solid white line with the companion star to scale. The colour scale depicts the amount of absorption (as $\exp(\tau_{\gamma\gamma})$).

References

[1] S. Johnston, R. N. Manchester, A. G. Lyne, et al., *PSR 1259-63: A Binary Radio Pulsar with a Be Star Companion A&A* **387** (1992) 37

[2] F. Camilo, P. S. Ray, S. M. Ransom, M. Burgay, et al., *Radio Detection of LAT PSRs J1741-2054 and J2032+4127: No Longer Just Gamma-ray Pulsars ApJ* **705** (2009) 1

[3] A. A. Abdo, M. Ackermann, M. Ajello, W. B. Atwood, et al., *Detection of 16 Gamma-Ray Pulsars Through Blind Frequency Searches Using the Fermi LAT Science* **325** (2009) 840

[4] C. D. Dermer, M. Böttcher, *Model for High-Energy Radiation from the Black-Hole Microquasar LS 5039 AAS* **207** (2005) 9007

[5] F. Jaron, R. Sharma, M. Massi, L. Fuhrmann, et al., *Radio QPO in the γ-ray-loud X-ray binary LS I +61°303 MNRAS* **471** (110)

[6] B. M. Gaensler, P. O. Slane, *The Evolution and Structure of Pulsar Wind Nebulae A&A* **44** (2006) 17

[7] G. Dubus, *Gamma-ray absorption in massive X-ray binaries A&A* **451** (2006) 9

[8] V. Bosch-Ramon, M. V. Barkov, *Large-scale flow dynamics and radiation in pulsar γ-ray binaries A&A* **535** (2011) A20

[9] V. Bosch-Ramon, M. V. Barkov, D. Khangulyan, M. Perucho, *Large-scale flow dynamics and radiation in pulsar γ-ray binaries A&A* **544** (2012) A59

[10] V. Zabalza, V. Bosch-Ramon, et al., *Unraveling the high-energy emission components of gamma-ray binaries A&A* **551** (2013) A17

[11] J. M. Jauch, F. Rohrlich, *Texts and Monographs in Physics* 2nd *ed.* **New York: Springer** (1967)

[12] M. Ribó, J. M. Paredes, G. E. Romero, et al., *LS 5039: A runaway microquasar ejected from the galactic plane A&A* **384** (2002) 954

[13] M. V. McSwain, D. R. Gies, W. Huang, et al., *The N Enrichment and Supernova Ejection of the Runaway Microquasar LS 5039 ApJ* **600** (2004) 927

[14] G. E. Sarty, T. Szalai, L. L. Kiss, et al., *The γ-ray binary LS 5039: mass and orbit constraints from MOST observations MNRAS* **411** (2011) 1293

[15] R. M. Shannon, S. Johnston, R. N. Manchester, *The kinematics and orbital dynamics of the PSR B1259-63/LS 2883 system from 23 yr of pulsar timing MNRAS* **437** (2014) 3255

[16] J. C. Miller-Jones, A. T. Deller, R. M. Shannon, et al., *The geometric distance and binary orbit of PSR B1259-63 MNRAS* **479** (2018) 4849

[17] I. Negueruela, M. Ribó, A. Herrero, et al., *Astrophysical Parameters of LS 2883 and Implications for the PSR B1259-63 Gamma-ray Binary ApJ* **732** (2011) L11

[18] C. Aragona, M. V. McSwain, E. D. Grundstrom, et al., *The Orbits of the γ-Ray Binaries LS I +61 303 and LS 5039 ApJ* **689** (2009) 514

[19] H. An, E. Belim, V. Bhalerao, et al., *Broadband X-Ray Properties of the Gamma-Ray Binary 1FGL J1018.6-5856 ApJ* **806** (2015) 166

[20] I. M. Monageng, V. A., McBride, L. J. Townsend, et al, *The Orbit of the Gamma-Ray Binary 1FGL J1018.6-5856 ApJ* **847** (2017) 68

[21] V. J. Napoli, M. V. McSwain, M. Viginia, et al., *The Distance of the γ-Ray Binary 1FGL J1018.6-5856 PASP* **123** (2011) 1262

[22] C. Aragona, M. V. McSwain, M. Virginia, M. De Becker, *HD 259440: The Proposed Optical Counterpart of the γ-ray Binary HESS J0632+057 ApJ* **724** (2010) 306

[23] J. Casares, M. Ribó, I. Ribas, et al., *On the binary nature of the γ-ray sources AGL J2241+4454 (= MWC 656) and HESS J0632+057 (= MWC 148) MNRAS* **421** (2012) 1103

[24] E. Aliu, S. Archambault, S., T. Aune, et al., *Long-term TeV and X-Ray Observations of the Gamma-Ray Binary HESS J0632+057 ApJ* **780** (2014) 168

[25] R. H. D. Corbet, L. Chomiuk, M. J. Coe, et al., *A Luminous Gamma-ray Binary in the Large Magellanic Cloud ApJ* **829** (2016) 105

[26] G. Pietrzyński, D. Graczyk, W. Gieren, et al, *An eclipsing-binary distance to the Large Magellanic Cloud accurate to two per cent Nature* **495** (2013) 76

[27] B. van Soelen, N. Komin, A. Kniazev, P. Väisänen, *The orbital parameters of the gamma-ray binary LMC P3† MNRAS* **484** (2019) 4347

[28] M. Böttcher, C. D. Dermer, *Photon-Photon Absorption of Very High Energy Gamma Rays from Microquasars: Application to LS 5039 ApJ* **634** (2005) 81

[29] H.E.S.S. Collaboration, et al., *Detection of variable VHE gamma-ray emission from the extra-galactic gamma-ray binary LMC P3 A&A* **610** (2018) L17